J Mater Sci (2007) 42:4435–4440
DOI 10.1007/s10853-006-0661-z

Effect of neodymium on microstructure and corrosion resistance of AZ91 magnesium alloy

Y. L. Song · Yao Hui Liu · S. R. Yu · X. Y. Zhu · S. H. Wang

Received: 6 March 2006 / Accepted: 10 July 2006 / Published online: 28 February 2007

Abstract The corrosion behavior of a new Mg–9Al–1Zn (AZ91) magnesium alloy containing neodymium (Nd) is investigated by scanning electron microscopy (SEM), X-ray diffraction (XRD), X-ray photoelectron spectroscopy (XPS), immersion tests and electrochemical experiments. The results indicate that Nd decreases the size and volume fraction of the β ($Mg_{17}Al_{12}$) phase and forms Al_2Nd in the alloy. In addition, during corrosion, Nd is incorporated into corrosion film in the form of Nd_2O_3. AZ91 alloy containing 1.0 wt.% Nd possesses an outstanding passivation property and excellent corrosion resistance. The corrosion resistance enhancement is attributed to the reduction in the size and volume fraction of the β phase and the incorporation of Nd_2O_3 in the corrosion film.

Introduction

Magnesium and its alloys, whose density is about one quarter of steel and two thirds of aluminium, have become promising materials for automobile industry in which weight saving pays many dividends [1, 2]. Among the various magnesium alloys, the Mg–9Al–1Zn (AZ91) alloy is most widely used because of its excellent castability and mechanical properties. However, the attractive advantages of the AZ91 magnesium alloy cannot expand further its current application level mainly due to its poor corrosion resistance. Rare earth elements have been widely used as alloying elements in magnesium alloys in order to modify their microstructures and improve their mechanical properties [3–7]. However, a limited number of publications in the field indicate that the effect of the rare earth addition on the corrosion resistance of the magnesium alloys has not yet been extensively studied [8, 9].

In the present study, a novel Nd-containing AZ91 magnesium alloy with excellent corrosion resistance is fabricated. The mechanism of corrosion resistance enhancement in the AZ91–*x*Nd alloys is discussed in terms of their microstructures and corrosion behaviors. It is expected that the preliminary results can be of significance in promoting the extensive application of magnesium alloys in automobile industry.

Experimental

Material preparation and microstructural observation

Commercial magnesium alloy AZ91 was employed as the modifying target. Rare earth element Nd, which was added at 0.1 and 1.0 wt.% levels, was introduced through the Mg–Nd master alloy. According to the chemical composition of commercial AZ91, the desirable amounts of pure Al and Zn were added into the alloys in order to maintain the compositional coherence. Alloying was carried out by melting in a crucible furnace under the protection of CO_2 + 0.5% SF_6 atmosphere. The chemical compositions of AZ91–*x*Nd

Y. L. Song · Y. H. Liu (✉) · S. R. Yu · X. Y. Zhu · S. H. Wang
Key Laboratory of Automobile Materials of Ministry of Education and Department of Materials Science & Engineering, Jilin University, No. 5988 Renmin Street, Changchun 130025, PR China
e-mail: liuyaohui2005@yahoo.com

alloys, which were measured by inductively coupled plasma atomic emission spectroscopy (ICPAES), are shown in Table 1. The microstructures of as-cast AZ91–*x*Nd magnesium alloys were investigated by scanning electron microscopy (SEM) and energy dispersive spectrum (EDS), and phases were identified by X-ray diffraction (XRD).

Immersion testing

Immersion corrosion experiments were carried out to measure the corrosion rates of the AZ91–*x*Nd magnesium alloys. The AZ91–*x*Nd magnesium alloys were cut into rectangular specimens with dimensions of 10 mm × 10 mm × 2 mm. All the specimens were polished successively on fine grades of emery papers up to 1,000 grit and cleaned by ethanol. The specimens were immersed in a 5 wt.% NaCl aqueous solution saturated with $Mg(OH)_2$ for up to 5 days. After immersion testing, corrosion products were removed by immersing the specimens in an aqueous solution of 20% CrO_3 + 1% $AgNO_3$ [10].

Electrochemical testing

Specimens for electrochemical testing were cut into cubes with dimensions of 10 mm × 10 mm × 10 mm. Each specimen was embedded in an epoxy resin with only one side unsealed. In this way, the working area exposed to the electrolyte was 10 mm × 10 mm in size. Before testing, these specimens were ground with 1,000-grit emery paper, washed by distilled water and dried by warm air. Potentiodynamic polarization curves were obtained in the 5% NaCl solution saturated with $Mg(OH)_2$ using a glass cell with the AZ91–*x*Nd magnesium alloy specimens as the working electrode. The counter electrode was a platinum gauze (25 mm × 25 mm in size, 52 mesh) and silver/silver chlorate electrode was used as the reference electrode. The potential was scanned from –1.6 V to –1.4 V at a rate of 1 mV/s.

Surface analysis

The corrosion film on the AZ91–1.0Nd magnesium alloy surface was obtained by immersing in the 5 wt.% NaCl aqueous solution saturated with $Mg(OH)_2$ for 24 h. Its composition was studied by X-ray photoelectron spectroscopy (XPS). Depth profiling was carried out using 3 keV Ar^+ ion sputtering.

Results

Microstructure

Figure 1a shows the typical features of the as-cast microstructure of the AZ91 magnesium alloy. The grains of primary α-magnesium solid solution are separated by the agglomerate β phase ($Mg_{17}Al_{12}$), which is one component of the totally divorced β-α-magnesium eutectic phases. Figure 1b shows the microstructure of the AZ91–1.0Nd alloy. The size of the α-magnesium grains is not significantly different from that in the AZ91 alloy, but both the size and the volume fraction of the β grains are apparently smaller. The β grains are homogeneously distributed along the boundaries of α-magnesium grains in the island-like particles. Alloying AZ91 with Nd leads to the formation of an additional phase, which is absent in the commercial AZ91 alloy. The precipitates, which can be easily distinguished by their light-white color, as opposed to the gray color of the $Mg_{17}Al_{12}$ precipitates, are uniformly scattered along the boundaries of α-magnesium grains in the fine particles with smooth edges because of similar solidification temperature to that of the β phases [11]. The XRD results (Fig. 2) indicate that the white precipitates in the modified alloy are Al_2Nd intermetallic compound. The EDS analysis (Table 2) reveals that Nd is dissolved in the α-magnesium and β grains in minute quantities in addition to the formation of the intermetallic compound. Obviously, the microstructure of the Nd-containing AZ91 is composed of primary α-magnesium solid solution, β–α eutectic phase containing Nd and Al_2Nd intermetallic compound.

Constant immersion

Figures 3 and 4 show the curves of weight loss and weight loss rate of the AZ91–*x*Nd alloys immersed in the 5% NaCl aqueous solution saturated with $Mg(OH)_2$ for 5 days. The weight loss of all the alloys

Table 1 Main compositions (wt.%) of the AZ91–*x*Nd alloys

Specimen	Al	Zn	Mn	Fe	Si	Nd	Mg	Impurity
AZ91	8.67	0.77	0.28	0.0008	0.019	–	Bal	<0.02
AZ91-0.1Nd	8.54	0.79	0.28	0.0005	0.019	0.11	Bal	<0.02
AZ91–1.0Nd	8.60	0.74	0.26	0.0005	0.018	1.02	Bal	<0.02

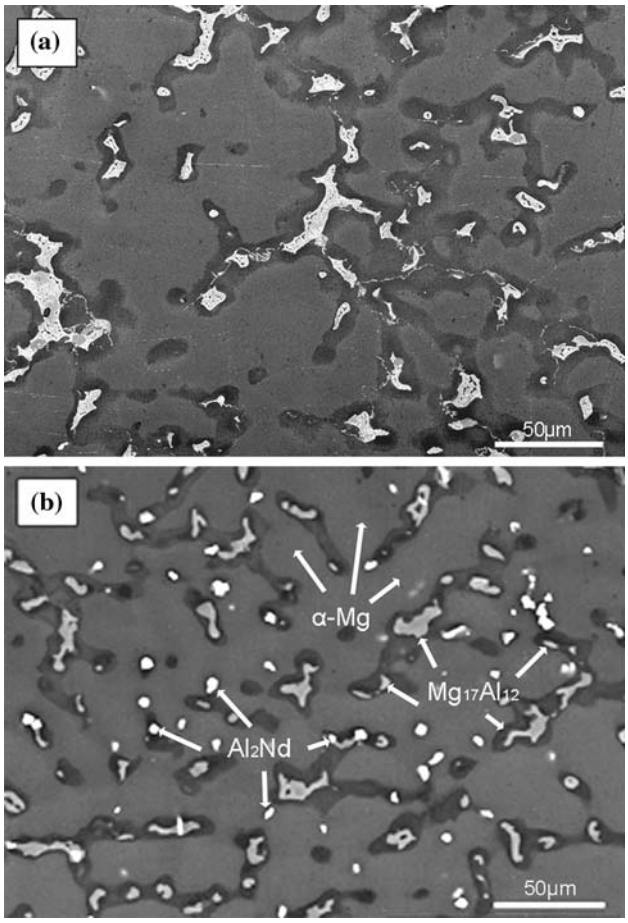

Fig. 1 SEM micrographs (SE mode) of as-cast AZ91–*x*Nd magnesium alloys: (**a**) AZ91 and (**b**) AZ91–1.0Nd

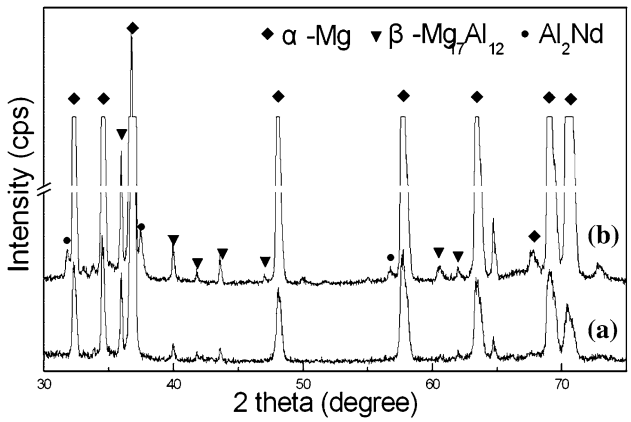

Fig. 2 XRD patterns of the AZ91–*x*Nd magnesium alloys: (**a**) AZ91 and (**b**) AZ91–1.0Nd

Table 2 EDS results of the α and β phases in the AZ91–1.0Nd alloys

Phase	Mg (wt.%)	Al (wt.%)	Zn (wt.%)	Nd (wt.%)
α	95.86	3.54	0.51	0.09
β	71.43	28.35	1.12	0.1

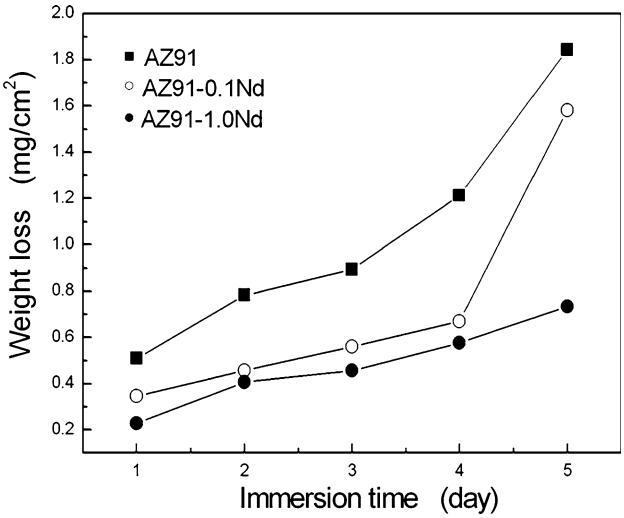

Fig. 3 Corrosion weight loss curves of the AZ91–*x*Nd alloys immerged in a 5% NaCl aqueous solution saturated with $Mg(OH)_2$ for 5 days

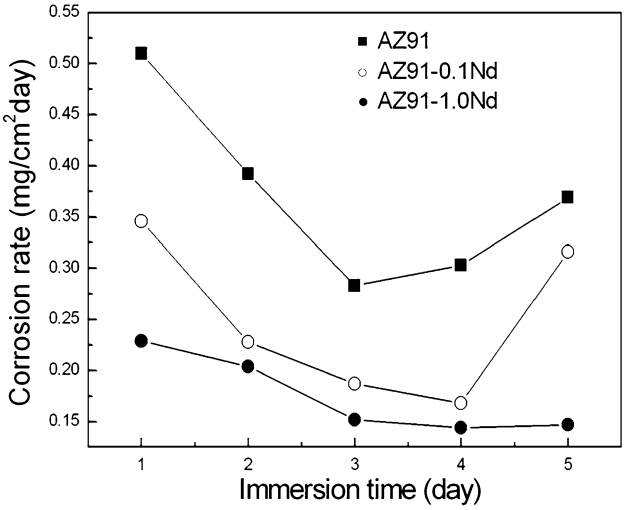

Fig. 4 Corrosion weight loss rate curves of the AZ91–*x*Nd alloys immerged in a 5% NaCl aqueous solution saturated with $Mg(OH)_2$ for 5 days

increases with the increase in time, but the values for the AZ91 alloy are always larger than those for the Nd-containing AZ91 alloy. Furthermore, the weight loss decreases with the increase in the Nd content at any time between 1 and 5 days. The corrosion rates of the three magnesium alloys in the specified time are diverse. The corrosion rate of AZ91 clearly decreases as the immersing time increases in the first 3 days. However, as the immersion time increases up to 4 days, the corrosion rate begins to increase. The corrosion rate curve of AZ91–0.1Nd is similar to that of AZ91 except for the longer duration during which the corrosion rate

decreases. The corrosion rate of AZ91–1.0Nd gradually decreases and then reaches a steady state as the immersion time increases. It is obvious that the AZ91–1.0Nd alloy exhibits better corrosion resistance in the immersion tests. The corrosion resistance of all the tested magnesium alloys can be ranked in ascending order: AZ91 < AZ91–0.1Nd < AZ91–1.0Nd.

Potentiodynamic polarization

Figure 5 shows the potentiodynamic polarization curves of the AZ91–*x*Nd magnesium alloys in the 5% NaCl aqueous solution saturated with $Mg(OH)_2$. It can be observed that the open circuit potential (OPC) of AZ91–0.1Nd is very close to that of AZ91. However, a further increase in the Nd content results in a significant shift of the OCP to a more positive value. Both cathodic and anodic curves of AZ91–1.0Nd are visually lower than that of AZ91. Moreover, the anodic curve of AZ91–1.0Nd is characterized by the passivation. Obviously, the Nd addition not only ennobles the OPC of AZ91, but also leads to a spontaneous passivation behavior. This result is in accordance with the immersion test, in which the Nd addition improves the corrosion resistance of the AZ91 alloy.

Surface analysis

Figure 6 shows the Mg 2p, Al 2p, O 1s and Nd 4d XPS depth profiling of the AZ91–1.0Nd alloy immersed in the 5% NaCl aqueous solution saturated with $Mg(OH)_2$ for 24 h. Figure 6a indicates that the oxidation products of Mg consist mainly of Mg oxide and hydroxide in the corrosion film. A component related to the metallic peak of magnesium is also present. Figure 6b reveals that both metallic Al and its oxide are in the corrosion film. The metallic Al is probably involved in the corrosion film during corrosion. The oxide and the hydroxide of Al exist in the outer layer but not in the inner layer of the film. The full width half maximum of the O 1s peaks shown in Fig. 6c is significantly broadened by surface charging, suggesting that the film of the AZ91–1.0Nd alloy contains the metallic oxides and hydroxides at the same time. Figure 6d reveals that the metallic Nd is incorporated into the corrosion film in the form of Nd_2O_3 during corrosion. The intensity of the BE (banding energy) peak of Nd_2O_3 at ~121 eV in the outer layer of the film is higher than that in the inner layer as a result of superposition of Nd_2O_3 and Al_2O_3 peaks. No Cl^- and CO_3^{2-} are found in the passive film by XPS due to their low content.

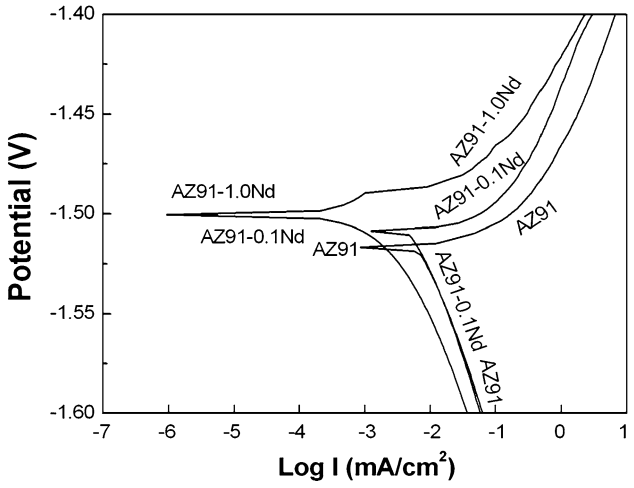

Fig. 5 Potentiodynamic polarization curves of AZ91–*x*Nd in a 5% NaCl aqueous solution saturated with $Mg(OH)_2$

Discussion

Microstructure

To some extent, the corrosion resistance of the AZ91 magnesium alloy depends on the morphology of the α-magnesium and β phases. Numerous researchers investigated the role of the α-magnesium and β grains in the corrosion, and have recognized that the β phase serves a dual purpose in the corrosion [12–17]. When the α grain size is small, the gaps between the β precipitates are narrow and the distribution of the β phase is nearly continuous. In this case, the β phase acts as a barrier to corrosion. On the other hand, if the α grain size is large and the β phase is discontinuously distributed along the boundaries of the α phases, the β phase acts as a galvanic cathode because of the larger potential difference between the α and β phases. Moreover, the galvanic corrosion is intensified if the area ratio of cathode to anode is greater. However, in the cast AZ91 alloy, due to the larger size of the α and β grains, the β phase serves as an active cathode during corrosion. The galvanic corrosion inevitably occurs owing to the galvanic current between the α and β phases. The Nd addition apparently decreases the size of the β phase and also reduces the volume fraction of the β phase in AZ91 by way of forming the Al_2Nd intermetallic compound, which reduces the eutectic reaction between the α and β phases by consuming Al in the alloys. The change in the microstructure of the Nd-containing AZ91 alloy decreases the cathode-to-anode area ratio during corrosion. As a consequence, the galvanic current density of the Nd-containing

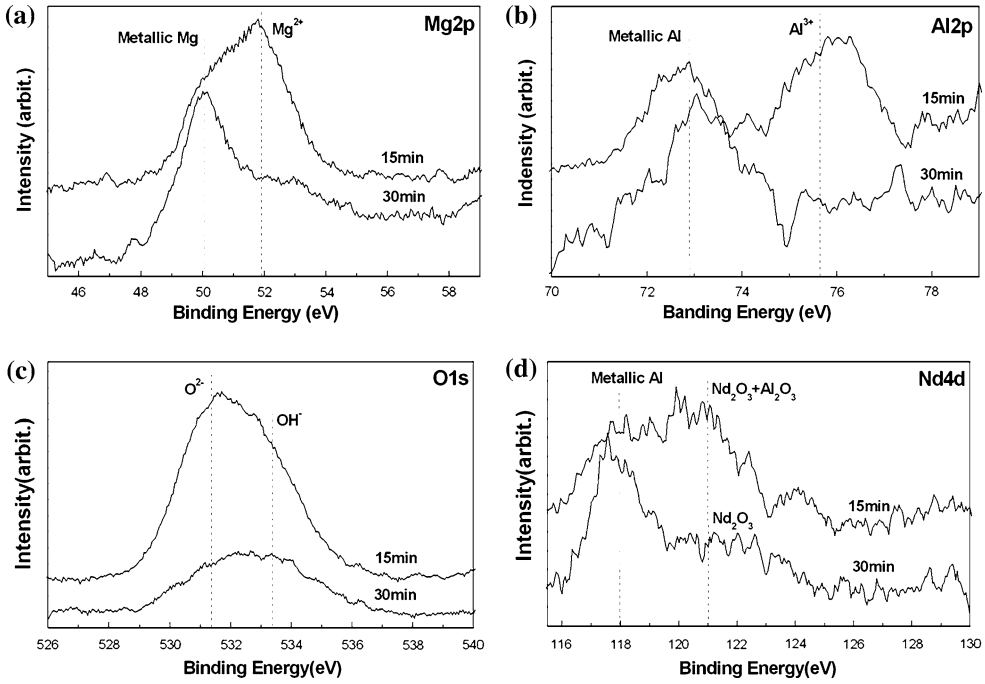

Fig. 6 Depth profiling XPS spectra of the surface film formed on AZ91–1.0Nd immersed in a 5% NaCl aqueous solution saturated with $Mg(OH)_2$ for 24 h: (**a**) Mg 2p, (**b**) Al 2p, (**c**) O 1s and (**d**) Nd 4d

AZ91 alloy is obviously reduced. In the Nd-containing AZ91 alloy, the Al_2Nd intermetallic compound behaves as a passive cathode over a wide pH range, although the potential of Al_2Nd is higher than that of the α phase [8]. The potentiodynamic cathodic polarization curve of AZ91–1.0Nd shows the same result (Fig. 5). It can be predicted that as a result of cathodic passivation, the current density of galvanic corrosion between the Al_2Nd intermetallic compound and the α phase is very low. In summary, as far as the change in the microstructure is concerned, the Nd addition is able to improve the corrosion resistance of AZ91 by decreasing the size and fraction of the β phase.

Surface film

The characteristics of surface films have a significant influence on the corrosion behavior. Improvement in the corrosion resistance can be expected by forming RE (rare earth) oxide in corrosion film on the magnesium alloy surface. Yao et al. [18, 19] observed that the corrosion film on the $Mg_{82-x}Ni_{18}Nd_x$ ($x = 5$, 15) alloys inhibited the penetration of the detrimental anions by trapping the Cl^- and CO_3^{2-} ions. The presence of the oxidized Nd was believed to be responsible for the significantly enhanced corrosion resistance of the $Mg_{82-x}Ni_{18}Nd_x$ alloys. Furthermore, the oxidation state of the RE element is very important for enhancing the passivity of the films. As for the Mg–Y alloys, the Y oxide was more effective in enhancing the passivity property of the alloys than the Y hydroxide. Rosalbino et al. [20] attributed the improved passivity of the Mg–Al–Er alloys to the incorporation of erbium in the corrosion film. Krishnamurthy [21] observed that the pseudo-passivation behavior of the rapidly solidified Mg–Y–Nd alloys was caused by the Y and Nd enrichment in the corrosion film. In the case of the AZ91–Nd alloys, metallic Nd is embedded in the corrosion film in the form of Nd_2O_3 formed during corrosion. The corrosion film containing Nd_2O_3 becomes more compact because the P–B ratio (the ratio of the oxide volume to the volume of the original element which was consumed to form the oxide) of the Nd oxide is greater than 1. It is beneficial to inhibit the penetration of the detrimental anions (Cl^-, CO_3^{2-}). Furthermore, the Nd oxide increases the local positive charge by substituting the magnesium cation. The increased positive charge is able to improve the corrosion resistance of the alloys on account of trapping the detrimental anions [18]. As a consequence, the Nd addition significantly improves the corrosion resistance of the AZ91 alloy partly due to its incorporation in the corrosion film in the form of Nd_2O_3.

Conclusions

1. The small addition of Nd to the AZ91 alloy effectively decreases both the size and the volume fraction of the β grain and also forms the Al_2Nd intermetallic compound that acts as a passive cathode during corrosion.

2. The change in the microstructure contributes to the improvement of the corrosion resistance of the AZ91 alloy.
3. During corrosion, Nd is oxidized to Nd_2O_3, which is incorporated into the corrosion film, and thereby enhances the corrosion resistance of the Nd-containing AZ91 alloys.

Acknowledgements This work was supported by The Program of Science and Technology Development in Jilin Province (No. 20040315) and ''985 project'' of Jilin University.

References

1. Ballerini G, Bardi U, Bignucolo R, Ceraolo G (2005) Corros Sci 47:2173
2. Song G, Atrens A, Stjohn D, Nairn J, Li Y (1997) Corros Sci 39:855
3. Avedesian MM, Baker H (1999) Magnesium and magnesium alloys. ASM International Material Park, USA, p 226
4. Lu YZ, Wang QD, Zeng XQ, Ding WJ, Zhai CQ, Zhu YP (2000) Mater Sci Eng A 278:66
5. Wang QD, Lu YZ, Zeng XQ, Ding WJ, Zhu YP, Li QH, Lan J (1999) Mater Sci Eng A 271:109
6. Pettersen G, Westengen H, Hoier R, Lohne O (1996) Mater Sci Eng A 207:115
7. Moreno IP, Nandy TK, Jones JW, Allison JE, Pollock TM (2003) Scr Mater 48:1029
8. Lunder O, Nisancioglu K (1993) Progress in the understanding and prevention of corrosion. The Institute of Materials, London, p 1249
9. Nordlien JH, Nisancioglu K, Ono S, Masuko N (1997) J Electrochem Soc 144:461
10. Song GL, Stjohn DH (2002) J Light Metals 2:1
11. Wei LY, Dunlop GL (1996) J Alloys Compd 232:264
12. Song GL, Bowles AL, Stjohn DH (2004) Mater Sci Eng A 366:74
13. Song GL, Atrens A, Wu XL, Zhang B (1998) Corros Sci 40:1769
14. Ambat R, Aung NN, Zhou W (2000) Corros Sci 42:1433
15. Lunder O, Lein JE, Aune TK, Nisancioglu K (1989) Corrosion 45:741
16. Song GL, Atrens A (1999) Adv Eng Mater 1:11
17. Song GL, Atrens A, Dargusch M (1999) Corros Sci 41:249
18. Yao HB, Li Y, Wee ATS, Pan JS, Chai JW (2001) Appl Surf Sci 173:54
19. Yao HB, Li Y, Wee ATS (2003) Electrochem Acta 48:4197
20. Rosalbino F, Angemini E, de Negri S, Saccone A, Delfino S (2005) Intermetallics 13:55
21. Krishnamurthy S, Khobaib M, Robertson E (1988) Mater Sci Eng 99:507